IEEE Access
Multidisciplinary | Rapid Review | Open Access Journal

Received August 11, 2020, accepted September 7, 2020, date of publication September 14, 2020,
date of current version September 24, 2020.

Digital Object Identifier 10.1109/ACCESS.2020.3023744

Allocation of FACTS Devices Using a Probabilistic Multi-Objective Approach Incorporating Various Sources of Uncertainty and Dynamic Line Rating

MAHROUS EL-AZAB[1], WALID A. OMRAN[2], SAID FOUAD MEKHAMER[3], AND HOSSAM E. A. TALAAT[3]

[1]Faculty of Engineering, Electrical Engineering Department, Ain Shams University, Cairo 11566, Egypt
[2]Electrical Engineering Department, Future University, New Cairo 11835, Egypt, on leave from Ain Shams University, Cairo 11566, Egypt
[3]Electrical Engineering Department, Future University, New Cairo 11835, Egypt

Corresponding author: Mahrous El-Azab (mahrousazab@yahoo.com)

ABSTRACT Flexible AC transmission system (FACTS) controller play an essential role in increasing the penetration level of renewable energy resources owing to their ability in continuously controlling the active and reactive power flow in the network. This paper presents a probabilistic multi-objective optimization approach to obtain the optimal sizes and locations of static var compensators (SVCs) and thyristor-controlled series capacitors (TCSCs) in a power transmission network with high penetration level of wind generation. The objective of the problem is to maximize the system loadability while minimizing the network power losses and the installation cost of the FACTS controllers. In this study, the uncertainties associated with wind power generation and the correlated load demand are considered. The uncertainties are handled in this work using the points estimation method. Moreover, the dynamic line ratings (DLRs) of the transmission lines are considered in this work. In this case, the maximum transmission capacity of transmission lines is estimated dynamically according to the weather conditions. Considering the DLRs or transmission lines is expected to avoid unrealistic congestion in the network, and hence, improve its loadability. The optimization problem is solved using the multi-objective teaching-learning based optimization (MO-TLBO) algorithm to find the best locations and ratings for the FACTS controllers. Additionally, a technique based on the fuzzy decision-making approach is employed to extract one of the Pareto optimal solutions as the best compromise. The proposed approach is applied on the modified IEEE 30-bus system. The numerical results demonstrate the effectiveness of the proposed approach and show that the maximum loadability limit of the study system increases when considering the DLR. This limit can be enhanced to 123.0% without FACTS controller and 137.0 %,130 % and 132.0% by SVC, TCSC and (SVC-TCSC) respectively.

INDEX TERMS Dynamic line rating, FACTS, multi-objective optimization, MOTLBO, probabilistic load flow, two points estimation method, uncertainty, wind power.

I. INTRODUCTION

The current growth in demand for electricity and rising population of the world are forcing electric utilities to take benefit of renewable energy sources. In addition, the interest in these sources increased because of the rising concerns about environmental pollution and due to the decreasing installation costs for these systems. One of the most widely used renewable energy source is the wind, where the global installed capacity of wind energy systems has reached 591GW in 2018 [1]. In general, wind farms are installed at locations with relatively high average wind speeds. This limits the locations suitable for installing wind farms which might also be non-optimal from the network capability perspective. Moreover, the fluctuations in the wind power pose technical challenges on the network operation. The network capability problem can be overcome by transmission network expansion or enforcement to allow for high penetration levels of wind power. However, this option might be unappealing as it requires long construction time, excessive investment cost and rigorous environmental agreements. ''The Energy Policy Act of 2005'' defined advanced transmission technology as

The associate editor coordinating the review of this manuscript and approving it for publication was Dragan Jovcic.

a technology that can improve the efficiency, reliability or capacity of new or existing transmission networks [2]. This report lists several developing transmission technologies that can rise the transmission capacity of the transmission network, including, FACTS, high-voltage DC technology, and advanced conductor and energy storage technologies.

Therefore, some new transmission technologies that can take advantage of the potential of existing transmission system are very attractive and are more likely to be widely applied in the real world [3]. In general, most transmission lines are planned and operated using the conventional static line rating (SLR). In this case, the ratings of the transmission system are limited based on the extreme weather conditions. This conservative approach may limit the full utilization of the transmission lines capacity [4]. Accordingly, transmission service providers are investigating alternative approaches that can efficiently utilize the transmission network. One of these approaches is the use of the DLR of transmission lines which depends on the real weather data to provide realistic loading conditions of the lines [5]. Therefore, this article will focus on the allocation problem of FACTS controllers while considering the DLR of transmission lines to improve the power system loadability in the presence of high penetration level of wind power.

FACTS controller can be installed to improve electric network performance [6]. Moreover, these devices can be used to mitigate the deleterious effects of wind power systems on the electric network, and thus, can be used to increase their penetration level [7]. The capability of FACTS controller in improving the network performance depends mostly on their sizes and locations [8]. Therefore, the proper installation of a FACTS controller at different locations in the network will give different results in terms of network loadability increase [9], loss reduction [6, 10], static voltage stability enhancement [11], voltage profile improvement [12], available transfer capability improvement [13] and total generation fuel cost reduction [14] and Congestion management [15]. From the literature survey, it is found that many researchers have suggested different methods to find optimum allocations of FACTS controller for optimization of one or two objectives with or without the presence of renewable energy.

Several studies considered the FACTS allocation problem as a single objective problem For example, coordination between SVC equipment and other FACTS controllers to achieve power flow management is presented in [16]. In addition, the optimal location and parameter setting of different FACTS, such as SVC, TCSC and thyristor-controlled phase angle regulator (TCPAR) shows that, a TCPAR is well in decreasing the total power loss, while the SVC is slightly well in the improvement of the voltage profile [7]. A hybrid evolutionary algorithm to optimally place multi-type FACTS controller to maximize the total transfer capability (TTC) [6] and Whale Optimization Algorithm, to optimally locate two TCSC for enhancing ATC [16]. The use of FACTS controller to achieve one specific objective while considering the uncertainties in the power system was considered in several studies. For example, the uncertainty of power systems was considered in [17] by applying Monte-Carlo simulation (MCS) technique for the sizing of various FACTS controllers. The objective of this study was to improve the voltage profile of the power network. The optimal allocation of FACTS controllers to minimize the cost of generation was solved in [18] by applying the differential evolution algorithm with MCS to consider the uncertainty in load and wind generation output.

In general, FACTS controller can be used to provide multiple services for the electric network. This can be achieved by formulating a multi-objective optimization problem which considers both the economical and technical aspects [19]. As an example, the work presented in [20] used the gravitational search algorithm to allocate the FACTS controllers for improvement the loadability of transmission network, reducing the active power losses and operation cost for different loading conditions. In [21], a multi-objective hybrid optimization approach to optimally allocate SVC and TCSC for the minimization of voltage deviation, voltage instability index and real power loss. In [22], a multi-objective framework was utilized to determine the optimal size and location of a unified power flow controller to maximize the system predictability and minimize the real power losses. In this study, the two-point estimating method (2PEM) was implemented to deal with the probabilistic nature of the wind power and loads. One common aspect of these studies is the consideration of the static line rating (SLR) of the transmission lines when solving the FACTS allocation problem.

The static line rating (SLR) is based on the line ampacity, which is calculated taking into account static weather conditions. For its computation worst case weather parameters are assumed so that the maximum flow current is obtained without violating temperature limits [4]. This way of operating the ratings does not consider a real-time analysis approach and often is excessively conservative. By under-utilizing the already built assets, with worst-case scenario conservative approaches, power networks are not being put into optimal usage and, therefore, are posing unnecessary compromises to both transmission system operators (TSOs) supply and electricity consumers demands. Naturally, it will be easy to assume that dynamic rates take into account real-time analysis: changing weather conditions, with a high significance on wind behavior/variability. DLR brings the actual ability to provide operators with overhead transmission lines, which can carry electricity anytime and anywhere according to their respective regional weather conditions. At the same time all design limits are being respected, such as conductor temperature [5]. This solution is of utmost interest of TSOs since by utilizing the existing assets in terms of transmission lines, the invested capital into this section is fairly diminished when comparing to rebuilding more resilient systems from scratch.

Clearly, the development of DLR technology has led to an increase in the capacity of existing transmission lines, which will eliminate the need for new transmission lines,

thereby contributing to the installation of renewable energy projects. Various studies and field tests have been conducted to analyze the potential benefits of DLR technology. This can help in using the full capability of the transmission network and therefore can provide an effective solution to the overload or congestion of the power network [23]. In [24], The economic benefits of implementing DLR on specific power systems with wind power generation capabilities are studied. The results show that the implementation of DLR can achieve more wind power, and the implementation of DLR can bring huge economic benefits. In [25] The potential reliability benefits of OHL and underground cable DLR in the distribution system are studied. The results not only show that DLR has brought significant reliability improvements, but also prove the fact that DLR has a greater impact on the enforcement of OHL than underground cables. Furthermore in [26] Sequential Monte Carlo (SMC) approach is used to assess the influence of DLR on power network reliability. The results show that higher reliability and greater wind power transmission can be improved. In [27] a stochastic transmission expansion plan including DLR was implemented, and DLR was verified to reduce the number of new transmission lines to be constructed. In terms of power system dispatching, DLR forecasting research makes it possible to consider this technology in the issue of day-to-day dispatching, so as to obtain a more economical dispatching scheme when the power market is deregulated. In [28], in the presence of wind energy integration, stochastic optimization is further applied to the security constraint unit commitment (SCUC) model. DLR has been verified to reduce wind power spillage.

In the literature, identifying the optimal locations and compensation degree of FACTS controller has been widely considered. Several techniques have been utilized to solve the FACTS controller allocation problem. These Methods can be divided into three classes: Meta-heuristic optimization methods, sensitivity-based methods and classical optimization methods [8]. Meta-heuristic optimization methods have become a recommended choice for solving complex mathematical models in power systems. In recent years, researchers have studied many meta-heuristic techniques, including genetic algorithm (GA), sine and cosine optimization algorithm (SCOA), particle swarm optimization (PSO), firefly swarm optimization, differential evolution (DE), simulated annealing (SA) approach and Artificial bee colony (ABC) etc. [29]. All algorithms based on swarm and evolutionary intelligence require the adjustment of control parameters, such as generation number, population size, elite number, etc. In addition, some algorithms also require their own specific tuning parameters [30]. Improper adjustment of the algorithm parameters can increase the computational effort of the algorithm or provide suboptimal solutions. Hence, the excessive number of algorithm parameters makes it difficult to obtain the optimal results without excessive computational effort. Du to this fact, Rao *et al.* presented the optimization of teaching and learning (TLBO) algorithm [31], [32] which requires only limited parameters. These parameters are the population size and generation number. Since the initial development of TLBO, researchers have proposed numerous variants of the algorithm to achieve high convergence speed and solution quality [33], [34]. The TLBO algorithm has been widely accepted by optimization researchers. Zou *et al.* recently conducted a comprehensive investigation into the study of the TLBO algorithm [35]. In this study, multi-objective teaching and learning optimization (MOTLBO) [36] was used to allocate FACTS equipment to the transmission system to achieve effective economic and technical operation of the power system.

A review of the literature reveals, to the best of the authors knowledge, that none of the studies focused on the installation of FACTS devices while considering the DLR of transmission lines to enhance the performance of the system in the presence of large wind farms. Thus, this study introduces an approach based on multi-objective function for solving the FACTS devices allocation problem considering a high penetration level of wind energy and incorporating uncertainties in the wind generation output and electrical demand. Moreover, the probabilistic line rating is considered as a dynamic constraint along with load correlation. To solve the FACTS controller allocation problem, the MOTLBO algorithm combined with PEM is used.

The outline of the article is as follows: Modeling of system uncertainties is provided in Section II. The correlation between uncertain parameters is offered in Section III. The points estimation method (2PEM+1) for the probabilistic power flow (PPF) is introduced in Section IV. The mathematical modeling of FACTS is presented in Section V. In Section VI, the problem formulation is explained. The MOTLBO algorithm is provided in Section VII, while the test system and case studies are presented in section VIII. Approach assessment is provided in Section IX. Finally, Section X outlines the conclusions of the paper.

II. MODELING OF UNCERTAINTIES

One of the fundamental features of modern electric power systems is the increase in uncertainties related to both load and renewable energy resources. Several approaches have been proposed to handling the uncertainties in the electric power system, and they can be generally classified into robust optimization approaches, probabilistic approaches and interval - set analysis. An updated review of numerous recent approaches can be found in [37], [38]. Robust optimization approaches model uncertainties as intervals and involve optimization problems to solve state boundaries. In interval set analysis, the uncertainty is demonstrated as an interval or set, and the interval set algorithm is used to estimate the boundary of the output. Probabilistic approaches model uncertain parameters as random variables with known probability density functions, and use analytical methods to propagate uncertainty or Monte Carlo simulation. In this study, the probabilistic approach is used as it is the most commonly used for handling the uncertainties in power systems..

1) PROBABILISTIC LOAD MODELING

The real and reactive power demands on the system are uncertain. they vary from instant to instant. This uncertainty can be modelled by considering the real and reactive power demands as probability distribution functions (PDF). Different PDFs can be used to represent this uncertainty in demand. However, the most accurate description is given by using gaussian or normal distribution function [39], [40]. The normal pdf is defined by two parameters mean (μ) and standard deviation (σ) of the uncertain variable can be defined mathematically as follows:

$$PDF\ (s) = \frac{1}{\sigma\sqrt{2\pi}} * exp^{\left(\frac{(-(S-\mu)^2)}{2\sigma^2}\right)} \tag{1}$$

where S represents apparent power of load, the load at each bus is demonstrated with mean (μ) equal to the base load and standard deviation (σ) is assumed to be $\pm$ 6 % of the base load [41].

2) PROBABILISTIC WIND MODELING

The power generated from wind turbines depends on the wind speed (v) which is usually modelled via the Weibull distribution PDF [39], [40].

$$PDF\ (v) = \left(\frac{k}{c}\right)\left(\frac{v}{c}\right)^{k-1} \exp\left[-\left(\frac{v}{c}\right)^{k}\right] \tag{2}$$

where c and k are the scale and shape factors of the Weibull function, respectively.

It is assumed that in each region, the PDF of wind speed is known, therefore, the transformation of wind speed to wind turbine output power is given by [41], [42]:

$$P\ (v) = \begin{cases} 0, & v \geq v_o or v \leq v_i \\ P_r\left(\dfrac{v - v_i}{v_r - v_o}\right), & v_i \leq v \leq v_r \\ P_r & v_i \leq v \leq v_o \end{cases} \tag{3}$$

where v_i, v_r and v_o are the cut-in, rated and cut-out wind speeds respectively, and P_r is the rated power.

3) PROBABILISTIC LINE RATING MODELING

The real maximum ampacity of the transmission lines can vary depend on a number of issues, Weather status like ambient temperature, solar radiation and wind speed and direction can influence conductor temperature and cause the capability variance on a line and throughout a day. What makes transmission line's capacity isn't a settled variable [43]. There are different methods that can be used to implement DLR, all involving different input parameters. These methods include [44]: 1) DLR forecasting using system loading and weather forecasting, 2) DLR estimation using indirect measurement 3) real-time DLR evaluation integrating actual meteorological data, which will be used in this work. Hence, it is necessary to consider line ampacity as probabilistic variables, where the PDF of the thermal limit (MVA) in the line corresponds to a generalized extreme value distribution [45] as shown in (4).

$$PDF\ (t) = (1/\sigma_l).\left(1 + \xi.\frac{(t-\mu l)^{\frac{-1}{\xi}}}{\sigma_l}\right).e^{\left(-\left(1+\xi\frac{(t-\mu l)}{\sigma_l}^{\frac{1}{\xi}}\right)\right)} \tag{4}$$

where t is the DLR of the line, μl is the location parameter, ξ is the shape parameter, and σ_l is the scale parameter. These parameters depend on the weather conditions and can be calculated based on [46]. Hence, the mean of the DLR is obtained for each period (e.g., season) and can be used as a constraint in the power flow equations.

III. CORRELATION BETWEEN UNCERTAIN VARIABLES

A. THE IMOORTANCE OF CORRELATION

Currently, due to serious environmental problems, the use of renewable energy for electrical energy production is growing rapidly. In this case, solar and wind energy are used most successfully. It is a well-known fact that there is a great correlation between these energies. This correlation may have a negative or positive impact on the operation of the power network [47]. In fact, it is actually possible to correlate the wind speeds of nearby wind farms proportionally. This problem may also lead to less / large wind power generation, which may seriously affect the power transmitted through the line. Similarly, this can happen to loads on certain buses. Weather conditions are one of the causal factors of this correlation. Therefore, it is very important to study the influence of the correlation of the power system.

As mentioned earlier, the correlation between uncertain variables plays a vital role in the future performance of the power grid. Therefore, the proposed probabilistic method for analyzing these networks must consider the correlation between uncertain input variables. System variables can depend on each other or not. Usually, this dependence is resolved by the correlation coefficient matrix or the covariance matrix [48]. The covariance matrix $\boldsymbol{V}$ can be calculated as:

$$V = \begin{bmatrix} \sigma_1^2 & \rho_{12}\sigma_1\sigma_2 & \ldots\ldots & \rho_{1m}\sigma_1\sigma_m \\ \rho_{21}\sigma_1\sigma_2 & \sigma_2^2 & \ldots\ldots & \rho_{2\mathrm{m}}\sigma_2\sigma_m \\ \ldots\ldots & \ldots\ldots & \ldots\ldots & \ldots\ldots \\ \rho_{\mathrm{m}1}\sigma_1\sigma_{\mathrm{m}} & \rho_{\mathrm{m}2}\sigma_{\mathrm{m}}\sigma_2 & \ldots\ldots & \sigma_m^2 \end{bmatrix} \tag{5}$$

where, σ is the standard deviation, ρ_{ij} is the correlation coefficient between the variables x_i and $x_j (i, j = 1, 2, 3, \ldots, k, i \neq j)$.

$V = LL^T$ is the covariance matrix, which is decomposed by Cholesky factorization [49], where L is the lower triangular matrix of V.

The correlation among the loads in the power network can be demonstrated using a correlated normal distribution function load (x_n) as follows [50]:

$$F\ (x_n) = \sqrt{\frac{1}{\sqrt{(2\pi)^m\ |V|}}} exp.\left((x-\mu)\ V^{-1}(x-\mu)\right) \tag{6}$$

where $\mu = [\mu_1, \mu_2, \mu_3, \ldots\ldots.., \mu_m]^T$, is expected value vector, m, is dimensional random input vector (x).

The random variables x, can be generated by transforming the generated samples from m-dimensional vector of typical normal random (x_n) using [50].

$$x = Lx_n + \mu \tag{7}$$

The correlation coefficient ρ_{ij} between all correlated loads is set as 0.7.

IV. PROBABLIISTIC POWER FLOW (PPF)

The deterministic power flow analysis relies on specific scenarios and ignores uncertainty within the parameters of the system and its states. On the other hand, a probabilistic approach evaluates the probability distribution for uncertain variables, and consequently, reflects realistic system performance more accurately. Several methods have been established for PPF analysis. These methods fall into three basic groups: analytical methods, MCS procedure, and approximation methods [37]. The PEM is currently one of the most popular of approximation methods used in PPF calculations. The PEM, like the MCS, makes use of a deterministic procedure to solve probabilistic problems but requires less computation effort [51]. One of the advantages of the PEM is that it requires the basic information of the random variables to be able to model them. This information includes the mean, variance, kurtosis, and skewness of the variables. In this work, the (2m+1) scheme is used as it takes the kurtosis of the input random variables into consideration while only one additional calculation is added to the function [52]. The scheme (2m+1) is applied to solve the PPF problem as follows:

$$\zeta\zeta_{l,k} = \frac{\lambda_{l,3}}{2} + (-1)^{3-k}\sqrt{\lambda_{l,4} - \frac{3}{4}\lambda_{l,3}^2} \quad k = 1, 2, {}_{l,3} = 0 \tag{8}$$

$$\zeta p_{l.k} = \mu_{pl} + {}_{l,k}\sigma_{pl} \quad k = 1, 2, 3 \tag{9}$$

$$\zeta\zeta\zeta w_{l.k} = \frac{(-1)^{3-k}}{m_{l,k}({}_{l,1} - {}_{l,2})} \quad k = 1, 2 \tag{10}$$

$$w_{l.3} = \frac{1}{m} - \frac{1}{m(\lambda_{l,4} - \lambda_{l,3}^2)} \tag{11}$$

where $\zeta_{l,k}$ is the standard location, μ_{p1}, σ_{pl} and $\lambda_{l,j}$ are the mean, standard deviation, and j^{th} standard central moment of the input random variables p_l. From (11), location $\zeta_{l,3} = 0$ yields $p_{l.3} = \mu_{pl}$ and so, of the locations are the same $(\mu_{p1}, \mu_{p2}, \ldots, \mu_{pl}, \ldots, \mu_{pm})$ point. Therefore, it is adequate to engage single calculation of the function at this location, given that equivalent weight w_0 as follows:

$$w_0 = 1 - \sum_{l=1}^{m} \frac{1}{m(\lambda_{l,4} - \lambda_{l,3}^2)} \tag{12}$$

Furthermore, (11) show that this scheme gives non-real locations when $\lambda_{l,4} - \frac{3}{4}\lambda_{l,3}^2$ is negative value. However, in power system problems the probability distributions are usually utilized to binomial, uniform, or normal model, therefore the locations are permanently real values.

To solve the PPF problem by (2m+1) scheme, the power flow input data are modeled as random variables, then the locations and weights are computed using (11) and (13). The solution of the PPF problem is [52]:

$$E\left(Z^j\right) = \sum_{l=1}^{m}\sum_{k=1}^{2} w_{l.k}\,(Z\,(l,k))^j + w_0 Z_0^j \tag{13}$$

$$(l,k) = F\left(\mu_{p1}, \mu_{p2}, \ldots, p_{l,k}, \ldots, \mu_{pm}\right), \quad k = 1, 2 \tag{14}$$

$$Z_0 = F\left(\mu_{p1}, \mu_{p2}, \ldots, \ldots, \mu_{pm}\right) \tag{15}$$

where $Z\,(l,k)$ is the output of the RVs related to the k^{th} concentration $\left(\mu_{p1}, \mu_{p2}, \ldots, p_{l,k}, \ldots, \mu_{pm}\right)$ of random variables, and introduces the relevance between the input and the output in the PPF. The gross number of deterministic PF to be run relies on the gathering scheme. The $Z\,(l,k)$ is apply to to assess the raw moments of the yield. the calculation closes when all centralizations of the all information RVs are considered. Then, the evaluated raw moments of the yield are utilized to calculate the required statistical data using (16).

V. FACTS MODELING

FACTS controllers are now considered one of the important and necessary devices to ensure the controllability, stability, power transfer capability, and durability of operating and transmitting energy in the in the power system. In this work, both the TCSC and SVC are used as the FACTS controllers. In general, the SVC can be used for voltage control, transient stability enhancement, and power factor correction. On the other hand, TCSC can be used to increase the steady state power flow limit.

A. SVC MODEL

The SVC, Fig. 1, is a FACTS device consisting of a shunt capacitor and reactor controlled statically by thyristor switches which is used to regulate the voltage at the installed bus [6]. The compensator is also able to damp power fluctuations. The magnitude of the reactive power rating of the SVC, Q_{svc}, can be determined using the SVC voltage, V_{svc}, and the SVC equivalent impedance, B_C, as follows:

$$Q_{SVC} = V_{SVC}^2 * B_c \tag{16}$$

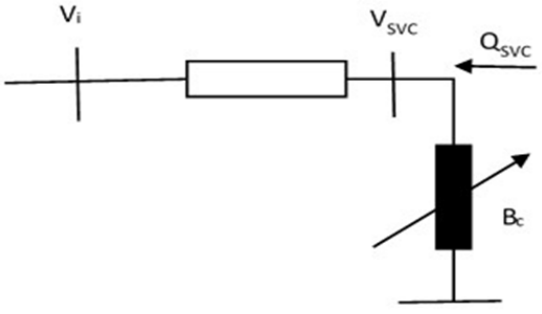

FIGURE 1. SVC steady state circuit representation.

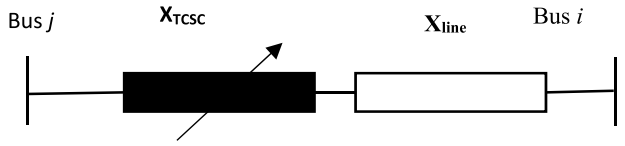

FIGURE 2. TCSC steady state circuit representation.

B. TCSC

The TCSC, Fig. 2, performances as a series-controlled reactance, which provides discrete control of the series line impedance. The TCSC controls the power flow in the system, which permits increasing the load of the existing grid. In addition, TCSC can damp the inter area oscillation of the large power systems and provide an opportunity for power flow modulation in response to different contingencies in the power system. Also The TCSC can modulate the steady-state power flow to retain it inside the lines thermal limits [53]. To guarantee the system stability, the series compensation of the line should be a percentage of the line nominal reactance value (X_{line}), This percentage can be inductive ($K_{se.ind}$) or capacitive ($K_{se.cap}$). As a result, the total branch reactance between Bus i and Bus j, (X_{ij}) is as follows:

$$X_{ij} = X_{line} + X_{TCSC}$$
$$K_{se,ind}X_{line} \leq X_{TCSC} \leq K_{se,cap}X_{line} \quad (17)$$

VI. PROBLEM FORMULATION

The optimal allocation of FACTS controller is formulated as mixed continues-discrete multi-objective optimization problem while satisfying numerous equality and inequality constraints. Generally, the problem can be expressed as follows.

A. OBJECTIVE FUNCTIONS

The multi-objective function for the allocation of SVC and TCSC to maximize the network loadability, minimize the active power loss, and minimize the installation cost can be formulated as:

$$Min.F\,(x,u) = \mathbb{E}\left[f_1\,(x,u)\,, f_2\,(x,u)\,, f_3\,(x,u)\right] \quad (18)$$
$$\text{subject to: } g\,(x,u) = 0$$
$$h\,(x,u) \leq 0 \quad (19)$$

where F is the vector of objective functions, f_1, f_2 and f_3 are the functions to be optimized, x is the dependent variables such as voltage and angle of load buses, and u is the control variables such as generator voltage, generator real power output, transformer - tap setting, T, and the rating and location of FACTS devices; E denotes the expected value.

The first objective function is used to maximize the network loadability without causing any violation in the bus voltages or branches loading. To achieve this goal, the load factor of the electrical network is increased in an iterative optimization procedure as follows [9]:

$$f_1 = -\lambda_f \quad (20)$$
$$\mathbb{E}[P_{Li}\left(\lambda_f\right)] = \lambda_f * [\mathbb{E}(P_{Li})] \quad (21)$$
$$\mathbb{E}\left[Q_{Li}\left(\lambda_f\right)\right] = \lambda_f * [\mathbb{E}(Q_{Li})] \quad (22)$$
$$\lambda_f \in [1, \lambda_f^{max}] \quad (23)$$

where λ_f and λ_f^{max} are the load factor by which both the active and reactive power loads can be increased and the maximum value of loading, respectively. P_{Li} and Q_{Li} are the active and reactive demand at load bus i, respectively.

The second objective is to minimize the system losses and can be formulated as [52]:

$$f_2 = \sum\nolimits_{l=1}^{nl} g_l[V_i^2 + V_j^2 - 2V_iV_j\cos\left(\delta_i - \delta_j\right)] \quad (24)$$

where nl, is the number of branches; g_l the conductance of branch l; $V_i\angle\delta_i$ and $V_j\angle\delta_j$ are the voltages at the buses i and j respectively.

The third objective is to minimize the FACTS device installation cost which can be calculated as follows:

$$f_3 = 1000{*}C * Q \quad (25)$$

where C is the cost of installation of FACTS devices in US$/kVAr, Q is the size of the FACTS device in MVAr. The cost of TCSC and SVC can be calculated according to the following formula [16]:

$$C_{SVC} = 0.0003Q^2 - 0.3051Q + 127.38 \text{ US\$/KVAr} \quad (26)$$
$$C_{TCSC} = 0.0015Q^2 - 0.7130Q + 153.75 \text{US\$/KVAr} \quad (27)$$

B. CONSTRAINTS

The constraints are divided into two groups; equality and inequality constraints as follows.

1) EQUALITY CONSTRAINTS

Active and reactive power injections at each bus as the equality constraints of optimal power flow (OPF) optimization problems incorporating wind farms are represented as the follows:

$$f_{Pi} = P_{gi} + P_{wi} - \lambda_f * P_{Li}, \quad i \in N_L \quad (28)$$
$$f_{Q_i} = Q_{gi} + Q_{wi} - \lambda_f * Q_{Li}, \quad i \in N_L \quad (29)$$

where, f_{Pi} and f_{Q_i} are active and reactive power injections at bus i, P_{gi}, Q_{gi} are the generator real and reactive powers at bus i, respectively, P_{wi}, Q_{wi} are the active and reactive powers production from the wind farm at bus i.N_L is a set of load buses.

2) INEQUALITY CONSTRAINTS

The active and reactive powers supplied by each generator and the generator voltage V_g are limited to their maximum and minimum values.

$$P_{gi}^{min} \leq \mathbb{E}(P_{gi}) \leq P_{gi}^{max}, \quad i \in N_G \quad (30)$$
$$Q_{Ggi}^{min} \leq \mathbb{E}(Q_{gi}) \leq Q_{gi}^{max}, \quad i \in N_G \quad (31)$$
$$V_{gi}^{min} \leq \mathbb{E}\left(V_{gi}\right) \leq V_{gi}^{max}, \quad i \in N_G \quad (32)$$

where, N_G is a set of generator buses.

The constraints of line flow limits, S_l, and voltages at load bus, V_L, are represented as:

$$V_{Li}^{min} \leq \mathbb{E}(V_{Li}) \leq V_{Li}^{max}, \quad i \in N_L \tag{33}$$

$$E(S_l) \leq S_l{}^{max}, \quad i \in nl \tag{34}$$

where S_l is power flow through the line and $S_l{}^{max}$ is loading limit, which is either the SLR or the DLR.

The rating of the SVC and TCSC are limited [16]:

$$-100MVAr \leq Q_{iSVC} \leq 100MVAr, \quad i \in N_{SVC} \tag{35}$$

$$-0.8X_{li} \leq X_{iTCSC} \leq 0.2X_{li}, \quad i \in N_{TCSC} \tag{36}$$

where N_{SVC} and N_{TCSC} are the number of FACTS devices used.

The load factor λ_f is controlled by its boundaries as

$$1 \leq \lambda_f \leq \lambda_f^{max} \tag{37}$$

C. CONSTRAINT HANDLING STRATEGY

The techniques used to manage the constraints in case of meta-heuristic optimization algorithms have a significant impact on the quality of the solutions. Many ways exist for considering constraint functions in optimization problems. According to [54] they can be classified in the following categories: Penalty functions, separation of constraints and objectives, repair algorithms, special representation and operators and hybrid methods. A different approach for constraint-handling is described in [55] for single-objective optimization and multi-objective optimization. According to the classification from [54] that is given above, it belongs to the category separation of constraints and objectives. The approach is based on preferring feasible over infeasible solutions but in contrast to the death penalty the existence of infeasible solutions is permitted [21]. More exactly, if comparing two vectors $\vec{u}$ and $\vec{v}$, $\vec{u}$ is considered better than $\vec{v}$ if:

1) Both solutions are feasible but $\vec{u}$ has a better performance concerning objective function value (s), meaning $f(\vec{u}) < f(\vec{v})$ or $\vec{u} \prec \vec{v}$ for single-objective or multi-objective optimization, respectively.

2) Both solutions are infeasible but $\vec{u}$ has a lower sum of constraint violation than $\vec{v}$.

3) $\vec{u}$ is feasible and $\vec{v}$ is not.

Using this approach, the original selection method is used if two feasible individuals are compared. A feasible solution is always preferred over an infeasible solution. In the comparison of two infeasible solutions, the one that is closer to the feasible space should win to direct the search towards the feasible region.

In this study, the constraint violations that are considered are violations of the branch flow and bus voltage limits which can be expressed as follows:

$$BLL = \begin{cases} 0; & if\ \mathbb{E}(S_l) \leq S_l^{max} \\ e^{\left[\Upsilon\left(1-\frac{\mathbb{E}(S_l)}{S_{L.}^{max}}\right)\right]}; & if\ \mathbb{E}(S_l) > S_l^{max} \end{cases} \tag{38}$$

$$VL = \begin{cases} 0; & if\ 1.1 \geq \mathbb{E}(V_{Li}) \geq 0.95 \\ e^{[\nu(1-E(V_{Li})]}; & otherwise \end{cases} \tag{39}$$

where BLL and VL are the branch loading and the line voltage level, respectively, and Υ and ν are small positive constants [56].

VII. SOLUTION APPROACH

A. MOTLBO

The teaching-learning based optimization (TLBO) technique depends on the influence of a teacher on the learners in class. Similar to other population-based techniques, it uses a population to arrive to a global solution. The process of TLBO is split into two phases. The first is the "Teacher Phase" which involves the learning of students from the teacher, who is assumed to be the best student. The second phase is the "Learner Phase" which involves the learning of students from interactions between them [36]. In the MOTLBO algorithm, we use an external archive to save the finest solution got so far. We use the non-dominated sorting concept used in NSGA-II [55] to select individuals on the better front in order to push the population to the Pareto front. At the same time, in order to maintain the diversity of current best solutions in external archives, the concept of crowding distance calculation in [57] is used.

1) TEACHER PHASE

In the "Teacher phase", the Teacher is considered the most learned student in the class. Therefore, at each iteration 'i', the best learned among the population will act as Teacher and denoted by M_{new} and tries to bring the mean of the class (M_i) towards his level. The solution is improved using the difference mean (DM_i) as follows [57]:

$$DM_i = rand(0, 1) * (M_{new} - T_f M_i) \tag{40}$$

$$T_f = round[1 + rand(0, 1)] \tag{41}$$

$$X_i^{new} = X_i^{old} + DM_i \tag{42}$$

where T_f is the teaching factor designed as integer either 1 or 2. The new value of X_i^{new} is accepted if it gives less value of cost function.

2) LEARNER PHASE

In addition to learning knowledge from the teacher, the students can also increase their knowledge by discussing and interrelating with other students. A student will learn additional information if the other students have more information than them. During this stage, the student X_i interrelates randomly with another student X_j in order to grow their information. In the case that X_j provides a better solution than X_i, X_i accepts it, otherwise they will keep it as it is [57].

$$X_i^{new} = \begin{cases} X_i^{old} + r\left(X_i - X_j\right) & if\ f(X_i) < f\left(X_j\right) \\ X_i^{old} + r\left(X_j - X_i\right) & if\ f\left(X_j\right) < f(X_i) \end{cases} \tag{43}$$

The MOTLBO termination criterion assumed here is that the procedure is paused when the greatest number of cycles are

achieved. The last arrangement of learns performed yield the Pareto optimal set through their target value [57].

B. BEST COMPROMISE SOLUTION (BCS)

As soon as the Pareto optimal solutions are generated, a single solution that provides best results from the planner's point view can be chosen. Otherwise, a compromise solution, BCS, that provide acceptable results for all objectives can be obtained. To obtain the BCS, a fuzzy decision-making approach is used in this work. In this case, the i^{th} objective function f_i is denoted by the membership function μ_i which can be expressed as [58].

$$\mu_i = \begin{cases} 1 & f_i \le f_{i,min} \\ \dfrac{f_{i,max} - f_i}{f_{i,max} - f_{i,min}} & f_{i,min} < f_i < f_{i,max} \\ 0 & f_i \ge f_{i,min} \end{cases} \tag{44}$$

where $f_{i,max}$ and $f_{i,min}$ are the extreme and lowest values of the i^{th} objective function amongst all non-dominated solutions, respectively. For the individually non-dominated solution k, the corresponding membership function μ^k is considered to be [58]:

$$\mu^k = \frac{\sum_{i=1}^{Nobj} \mu_i^k}{\sum_{k=1}^{m} \sum_{i=1}^{Nobj} \mu_i^k} \tag{45}$$

where m is the number of Pareto solutions. Finally, the BCS is the one that achieves the greatest membership function μ^k [58].

C. PROBOASED APPROACH

The optimal allocation of SVC and TCSC devices is expressed as a hybrid continuous-discrete multi-objective problem (MOP). The optimization approach can be split into two levels. In the upper level, the MOTLBO seeks the best solution amongst several feasible solutions for the locations and ratings of FACTS controllers. The result of this level is sent to the second level where the (2PEM+1) method is used in the solution of the probabilistic OPF problem. This is an essential step for the estimation of the fitness function for each learner in the MOTLBO. The flowchart of the planned approach is shown in Fig.3. The proposed (MOTLBO/2PEM+1) step-by-step strategy is described as follows:

Step 1: The power network data, wind data, and MOTLBO parameters are entered.

Step 2: The rating and location of FACTS controller as well as control variable are set as the design variables.

Step 3: The first population (learners) is initialized as indicated by the number of design parameters and population size.

Step 4: The line data (for TCSC), bus data (for SVC devices) are calculated for each Learner Phase and probabilistic OPF is employed using the (2PEM+1) process to estimate the values of the objective functions for each learner.

Step 5: The constraint handling strategy is applied.

Step 6: Non-dominated results, if detected, are stored in the external archive.

Step 7: The mean value of the learners is calculated from this archive.

Step 8: The Teacher phase of the MOTLBO algorithm is run by randomly selecting the one of the non-dominated solutions to act as a teacher.

Step 9: The individual is modified based on the teacher using equations (41) to (43).

Step 10: The fitness value of the objective functions for each learner is calculated using the (2PEM+1).

Step 11: Non-dominated solutions are detected if present and the archive is updated.

Step 12: The Learner Phase of the algorithm is engaged and the positions of the learners is modified if they were improved by applying (44).

Step 13: Non-dominated individuals are detected if present and the archive is updated.

Step 14: If the termination rule is satisfied, Step 15 is executed, otherwise, the procedure loops back to Step 4.

Step 15: The expected value of the objective function is computed along with the size and locations of FACTS devices.

Step 16: The Fuzzy approach is applied to obtain the BCS.

Step 17: The procedure is terminated

VIII. TEST STSTEM AND CASE STUDIES

In order to validate the performance of the proposed MOTLBO approach is tested on a modified IEEE 30-bus. The operating conditions of the system is obtained from [59], [60] which is considered as the base case. It is assumed that there are two variable speed wind farms connected at bus 14 and 19, as shown in Fig. 4. Each farm has 24 identical wind turbines, with the following turbine parameters: NEG Micon 1500/64 wind turbine, $V_i = 5$ m/sec, $V_r = 15$ m/s, $V_o = 25$ m/s and $P_r = 1.5$ MW at unity p.f. The scale and shape parameters for the site is c = 8.549 m/s and k = 1.98, respectively. On all optimization runs, the initial control parameters for the MOTLBO, algorithm are set as maximum number of iterations (GN) = 200, Population size (N) = 100, The maximum size of the Pareto-optimal front was selected as 30 solutions.

A. CASE ONE: WITHOUT FACTS CONTROLLER

In this case, no FACTS equipment's are installed and the load factor λ_f is between [1, 1.5]. The objective of this case is to check the effect of DLR on the loadability and losses of the system. The problem was formulated as an MOP for power loss minimization and loadability maximization using MOTLBO. The results shown in Fig. 5 show the Pareto optimal solutions that the satisfy the constraints for both SLR and DLR. Based on the Pareto optimal solutions, the maximum system loadability (MSL), the best minimum power loss performance, the BCS and the optimum control variables can be obtained as shown in Table 1. It can be noted that for the BCS obtained using the using fuzzy min-max approach has,

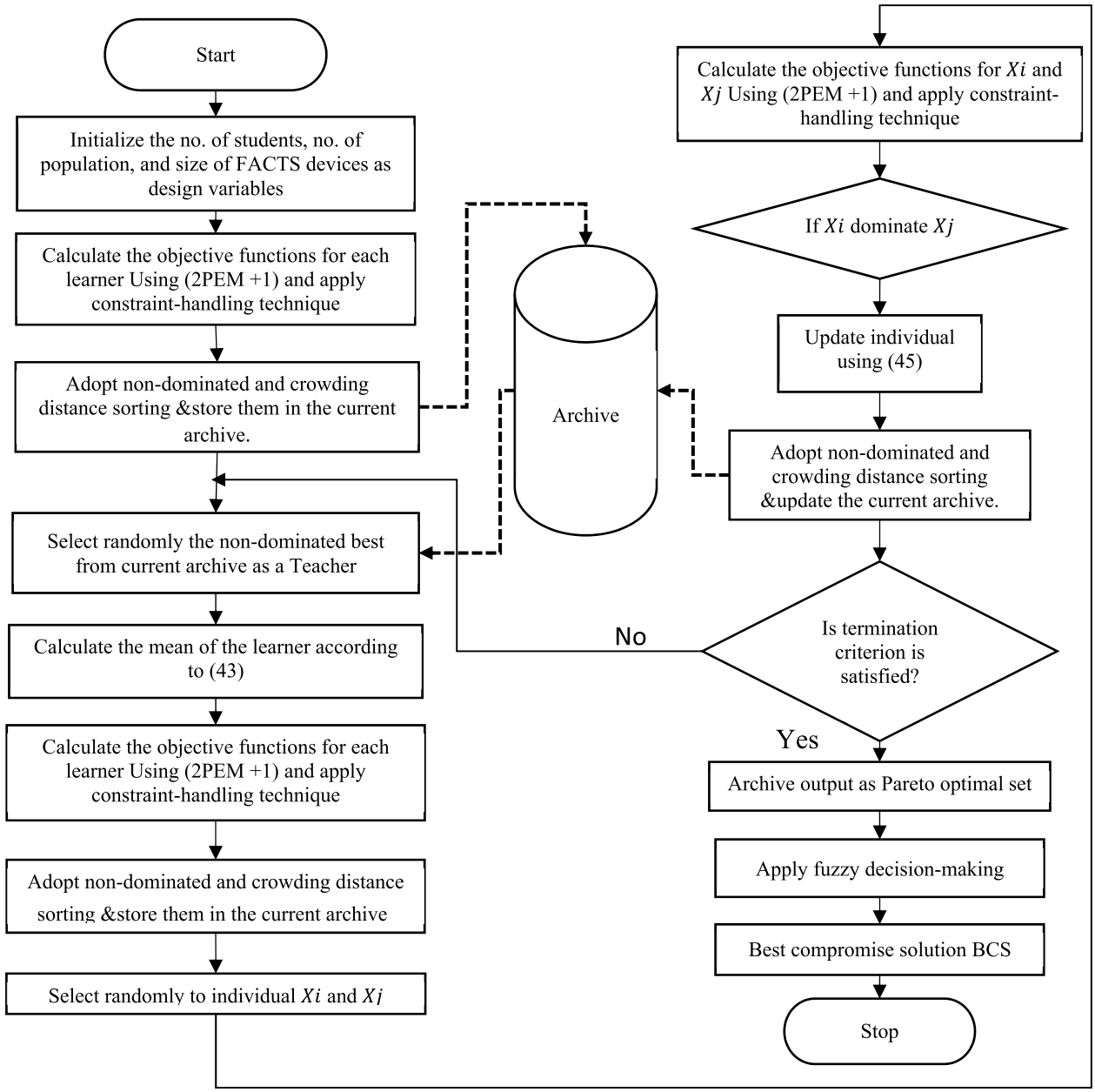

FIGURE 3. Flowchart of proposed algorithm for FACTS controllers allocation.

the system loadability of 112 % and the total transmission losses of 4.13 MW. In case of DLR, the system loadability of 123 % and the total transmission losses of 5.93 MW. Therefore, the use of SLR is a conservative approach that might limit the MSL without need, also, it can be seen when consider the DLR the line flow can be increased if compared with SLR as shown in Fig. 6, without violation thermal limit constraint.

B. CASE TWO: WITH FACTS CONTROLLER

In this case, the use of FACTS controllers to enhance the operation of the system is investigated considering the DLR. To achieve this task, three different scenarios are considered as follows: Scenario 1, three SVCs are to be installed, Scenario 2, one TCSC device is to be installed, finally, Scenario 3, three SVCs and one TCSC are to be installed. The three objectives considered in this case are similar to Case 1 with the addition of a third objective representing the minimization of the FACTS establishment cost.

1) SCENARIO 1

The diversity of the Pareto optimal solutions over the trade-off surface for this scenario in case of SLR and DLR are shown in Figs. 7 (a) and 7(b), respectively. Table 2

TABLE 1. Simulation results for objective function values and Optimum control variables for case one.

Control Variable & Objective	Min.	Max.	SLR			DLR		
			Best MSL	Best Losses	BCS	Best MSL	Best Losses	BCS
P_{g_2} MW	20.0	80.0	76.16	79.60	75.27	79.98	80.0	80.0
P_{g_5} MW	15.0	50.0	48.91	49.85	49.75	49.92	50.0	50.0
P_{g_8} MW	10.0	35.0	35	34.99	34.99	33.63	34.91	34.90
P_{g_11} MW	10.0	30.0	28.15	27.88	28.04	29.86	29.78	29.85
P_{g_13} MW	12.0	40.0	17.81	15.38	17.71	12.00	13.18	15.07
V_{g_1} (pu)	0.95	1.10	1.049	1.038	1.053	1.042	1.032	1.036
V_{g_2} (pu)	0.95	1.10	1.045	1.039	1.043	1.019	1.025	1.024
V_{g_5} (pu)	0.95	1.10	1.003	1.011	1.014	1.007	0.993	0.991
V_{g_8} (pu)	0.95	1.10	1.033	1.024	1.018	1.025	1.011	1.021
V_{g_11} (pu)	0.95	1.10	1.069	1.050	1.070	1.072	1.090	1.089
V_{g_13} (pu)	0.95	1.10	1.096	1.094	1.095	1.014	1.066	1.085
$T_{6\text{-}9}$ (pu)	0.90	1.10	0.986	1.0115	1.011	1.056	0.987	0.969
$T_{6\text{-}10}$ (pu)	0.90	1.10	0.900	0.956	0.900	0.939	0.921	0.956
$T_{4\text{-}12}$ (pu)	0.90	1.10	0.965	0.913	0.977	0.948	0.912	0.9247
$T_{27\text{-}28}$ (pu)	0.90	1.10	0.9129	0.916	0.911	0.919	0.911	0.928
λ_f	1.00	1.50	1.31	1.01	1.12	1.44	1.03	1.23
MSL (%)			**131.0**	101.0	**112.0**	**144.0**	103.0	**123.0**
$\mathbb{E}$ [Loses (MW)]			7.167	**3.02**	**4.135**	10.79	**2.93**	**5.93**

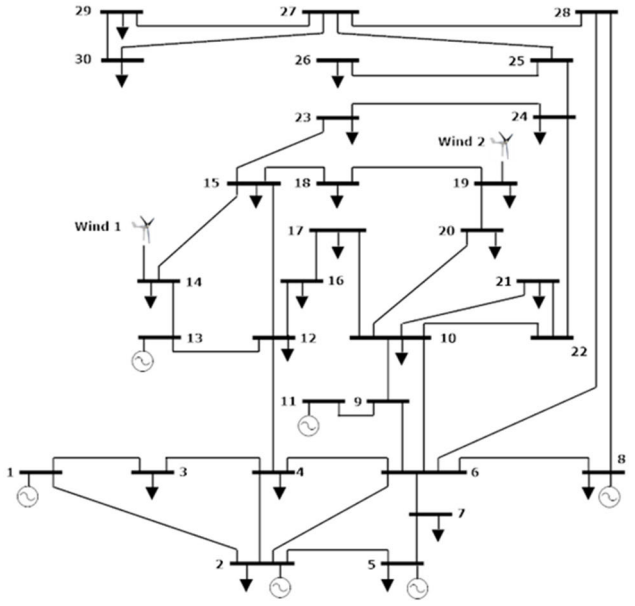

FIGURE 4. Modified IEEE 30-bus System.

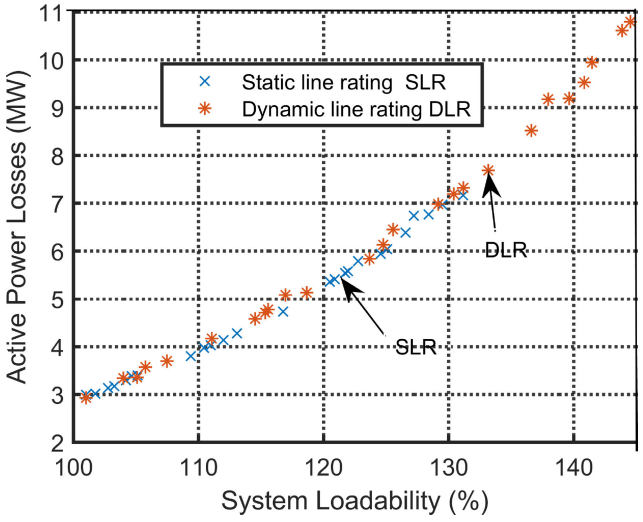

FIGURE 5. Pareto optimal front in two objective functions without FACTS controllers.

shows the optimum control variables, the optimal ratings and locations of the three SVCs as well as the corresponding best MSL, best expected real power loss, the FACTS establishment cost and the BCS. By using MO-TLBO algorithm, all the objectives, are optimized simultaneously and the best-compromised solution has been determined by using fuzzy min-max approach. In case of SLR, the obtained best-compromised solution has the SVCs are installed at

TABLE 2. Simulation results for objective function values AND OPTIMUM control variables FOR SCENARIO one (With SVC).

Control Variable & Objective	Min.	Max.	SLR				DLR			
			Best MSL	Best Losses	Best Cost	BCS	Best MSL	Best Losses	Best Cost	BCS
P_{g_2} MW	20	80	68.93	61.92	79.36	79.36	52.92	62.16	66.552	71.68
P_{g_5} MW	15	50	36.53	37.56	38.61	38.61	50	49.82	49.87	49.82
P_{g_8} MW	10	35	24.61	33.83	34.23	34.23	30.92	19.86	10.0	35.0
P_{g_11} MW	10	30	27.28	24.76	30.0	30.0	30	27.25	27.48	28.87
P_{g_13} MW	12	40	12.13	16.44	12.02	12.02	20.41	27.73	25.01	30.39
V_{g_1} (pu)	0.95	1.10	1.00	0.998	1.005	1.005	1.020	1.039	1.006	1.014
V_{g_2} (pu)	0.95	1.10	1.014	1.005	1.006	1.006	1.026	1.025	1.020	1.028
V_{g_5} (pu)	0.95	1.10	0.939	0.9612	0.953	0.953	1.008	0.993	0.9967	1.005
V_{g_8} (pu)	0.95	1.10	0.954	0.991	0.984	0.984	0.953	0.992	0.988	0.996
V_{g_11} (pu)	0.95	1.10	1.071	0.990	0.966	0.966	1.007	0.986	0.98245	1.086
V_{g_13} (pu)	0.95	1.10	0.976	0.990	1.006	1.006	1.056	1.050	1.038	1.010
$T_{6\text{-}9}$ (pu)	0.90	1.10	1.05	1.060	1.079	1.079	0.9451	1.021	0.974	1.0131
$T_{6\text{-}10}$ (pu)	0.90	1.10	0.930	0.921	0.927	0.927	0.9395	0.900	0.991	0.940
$T_{4\text{-}12}$ (pu)	0.90	1.10	1.030	1.042	1.006	1.006	0.9666	0.922	1.045	1.100
$T_{27\text{-}28}$ (pu)	0.90	1.10	0.930	0.952	0.9146	0.9146	0.9000	0.967	0.910	0.900
λ_f	1.0	1.50	1.31	1.01	1.07	1.17	1.35	1.01	1.25	1.37
MSL (%)			**131.0**	101.0	107.0	**117.0**	**135.0**	101.0	125.0	**137.0**
$\mathbb{E}$ [Loses (MW)]			9.81	**3.81**	4.96	**5.73**	11.21	**4.20**	9.12	**9.12**
ICX10^6 USD	-		1.92	1.006	**0.230**	**0.814**	2.49	1.11	**0.312**	**5.11**
SVC_1 (MVAr)	-100	100	5.97	2.67	0.535	2.72	-10.15	0.621	-0.186	16.24
SVC_2 (MVAr)	-100	100	6.15	1.09	0.561	2.13	3.84	-7.40	-1.430	24.93
SVC_3(MVAr)	-100	100	3.14	4.19	0.713	-1.57	5.98	-0.852	-0.842	1.03
Location Bus			30;25;9	3;17;6	3;20;6	30;14;4	7;16;3	10;3;15	12;3014	18;12;22

* Bold values represent the best results

in buses 30, 14, and 4, with ratings of 2.72, 2.13, and -1.57 MVAR, respectively. In this case the MSL is 117%, the power losses is 5.735 MW and the SVC establishment cost is US$ 0.814 $\times$ 10^6.

In case of DLR, the obtained best-compromised solution has the MSL is 137% with the SVCs installed at buses 18, 12, and 22 rated at -16.24, 24.93, and 1.03 MVAR, respectively. The losses has increased to 9.122 MW and the establishment cost of the FACTS equipment's has increased to US$ 5.114 $\times$ 10^6. This increase is due to the increase in the MSL.

2) SCENARIO TWO

The Pareto optimal solutions for this scenario in case of SLR and DLR are shown in Figs. 8 (a) and 8(b), respectively. Table 3 shows the optimum ratings and locations of the TCSC as well as the corresponding MSL, expected real power loss, the FACTS establishment cost and the BCS. In case of SLR, the TCSC are installed in line number 25 between

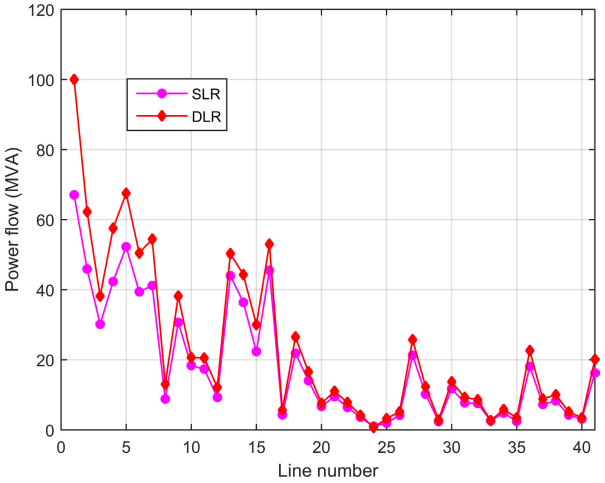

FIGURE 6. Power flow of IEEE 30-bus system with SLR and DLR.

buses (10-20), with rating of – 0.72 pu, based on the BCS. In this case the MSL is 125%, the power losses is 6.46 MW and the TCSC establishment cost is US$ 02.67 $\times$ 10^6.

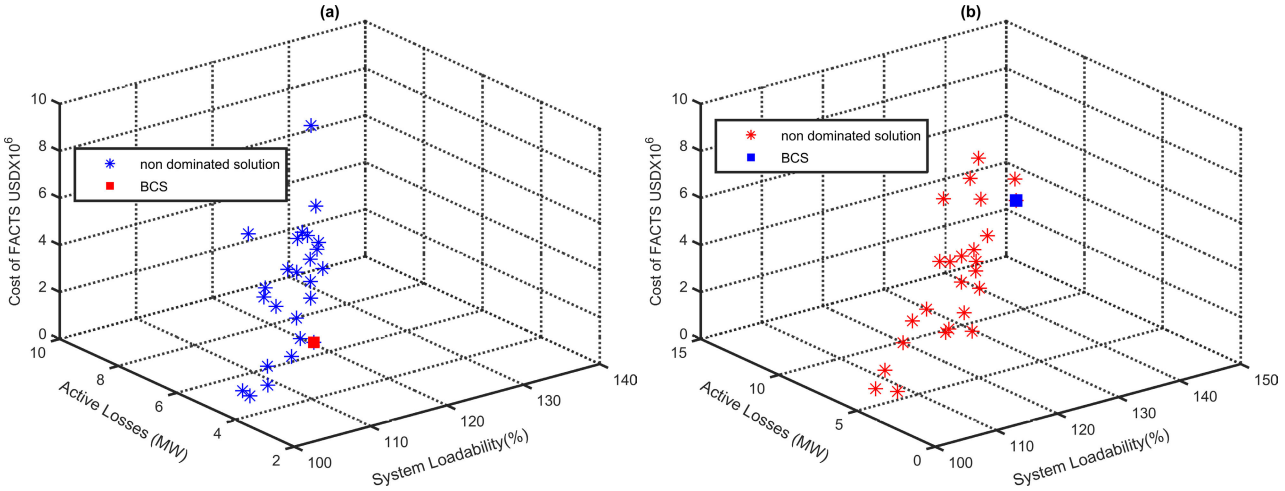

FIGURE 7. Pareto optimal set for allocation of SVC (a) SLR, (b) DR.

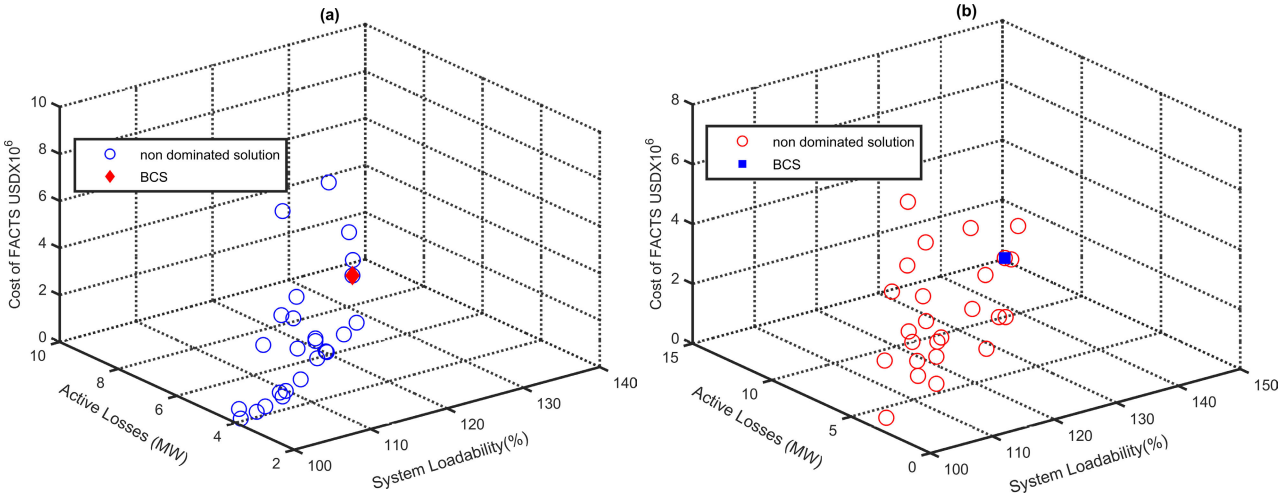

FIGURE 8. Pareto optimal front for allocation of TCSC (a) SLR, (b) DLR.

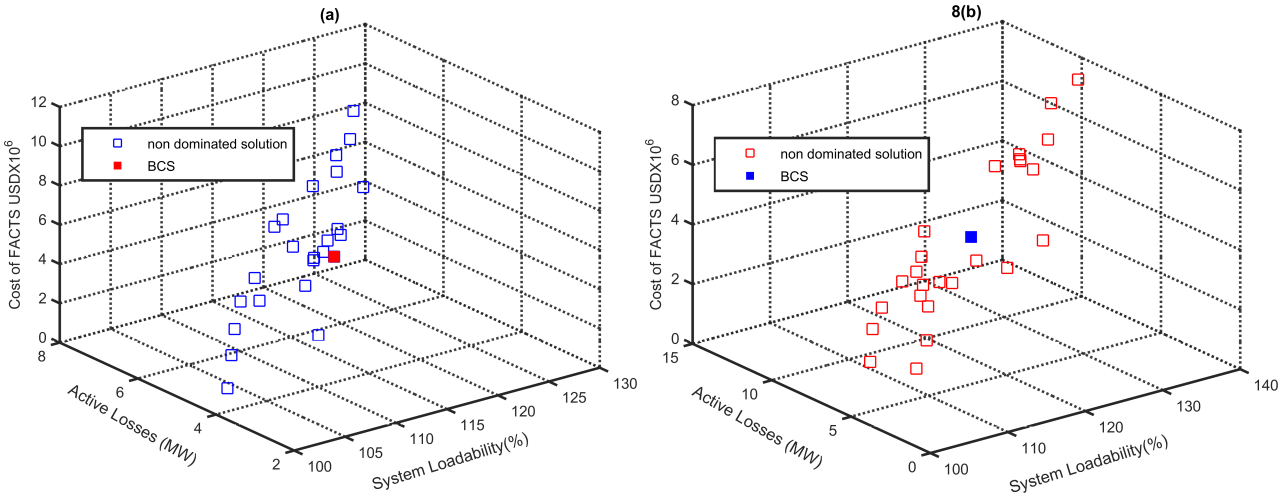

FIGURE 9. Pareto optimal front for rating and location of (TCSC-SVC) a (SLR), b (DLR).

In case of DLR, the obtained best-compromised solution has the MSL is increased to 130% with the TCSC installed in line number 16, between buses (12-15), with rating of –0.69 pu, the losses has increased to 7.06 MW and the establishment cost of the FACTS devices has increased to US$ 3.107×10^6.

TABLE 3. Simulation results for objective function values and Optimum control variables for scenario one (With TCSC).

Control Variable & Objective	Min.	Max.	SLR				DLR			
			Best MSL	Best Losses	Best Cost	BCS	Best MSL	Best Losses	Best Cost	BCS
P_{g_2} MW	20.0	80.0	78.72	78.20	79.79	80.00	73.31	69.33	70.260	75.45
P_{g_5} MW	15.0	50.0	48.35	46.91	50.00	49.38	49.71	48.18	48.690	47.13
P_{g_8} MW	10.0	35.0	33.93	35.0	35.00	34.26	19.66	34.75	30.36	35.00
P_{g_11} MW	10.0	30.0	30.0	29.79	29.69	30.00	29.22	29.83	30.00	29.455
P_{g_13} MW	12.0	40.0	12.0	29.36	35.52	26.66	16.41	36.66	40.00	40.00
V_{g_1} (pu)	0.95	1.10	1.043	1.026	1.021	1.050	1.053	1.060	1.05	1.047
V_{g_2} (pu)	0.95	1.10	1.017	1.032	0.999	1.028	1.063	1.048	1.072	1.031
V_{g_5} (pu)	0.95	1.10	0.993	0.998	0.950	0.988	1.038	1.020	1.035	0.997
V_{g_8} (pu)	0.95	1.10	1.001	1.005	0.980	1.001	1.000	1.035	1.040	1.033
V_{g_11} (pu)	0.95	1.10	1.020	1.044	1.016	1.086	1.041	1.011	1.067	1.077
V_{g_13} (pu)	0.95	1.10	1.044	1.049	1.026	1.079	1.070	1.082	1.039	1.073
$T_{6\text{-}9}$ (pu)	0.90	1.10	1.094	0.9903	1.095	0.994	0.963	0.981	1.0473	0.997
$T_{6\text{-}10}$ (pu)	0.90	1.10	0.900	0.9109	0.900	0.923	0.900	0.902	0.9000	0.900
$T_{4\text{-}12}$ (pu)	0.90	1.10	1.097	1.0137	1.001	1.015	1.095	1.0291	1.053	0.9522
$T_{27\text{-}28}$ (pu)	0.90	1.10	0.968	0.940	0.900	0.900	0.952	0.944	0.900	0.922
λ_F	1.0	1.50	1.31	1.01	1.03	1.25	1.5	1.01	1.28	1.3
MSL (%)			**131.0**	101.0	103.0	**125.0**	**150.0**	101	128.0	**130.0**
$\mathbb{E}$ [Loses (MW)]			8.30	**3.315**	4.565	**6.46**	14.01	**3.28**	7.33	**7.06**
ICX10^6 USD	-		2.88	3.612	**0.0277**	**2.76**	1.36	2.24	**0.132**	**3.107**
TCSC (pu)	-0.2	0.8	-0.663	-0.586	-0.80	-0.72	-0.694	-0.735	-0.592	-0.690
Location Bus			12-13	9-11	15-23	10-20	12-14	10-17	15-18	12-15

* Bold values represent the best results

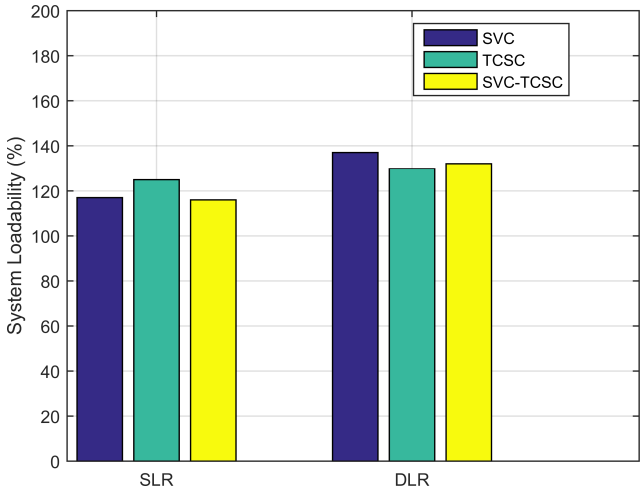

FIGURE 10. MSL (%) comparison for SLR and DLR for different FACTS controllers.

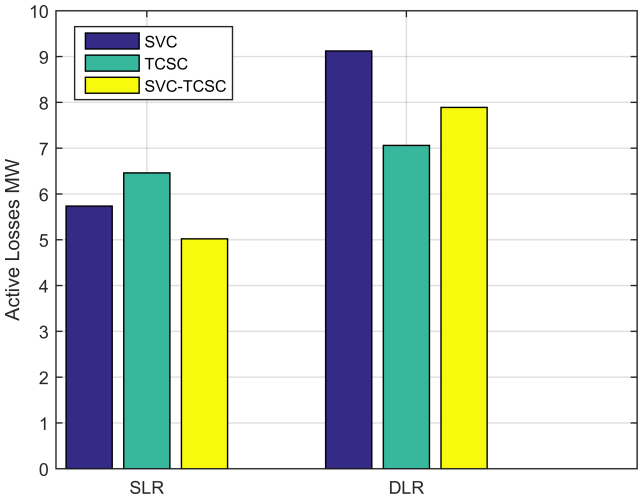

FIGURE 11. Active power losses (MW) comparison for SLR and DLR for different FACTS controllers.

3) SCENARIO THREE

The Pareto optimal solutions for this scenario in case of SLR and DLR are shown in Figs. 9 (a) and 9(b), respectively. Table 4, shows the optimal ratings and locations of the three SVC and one TCSC as well as the corresponding MSL, expected real power loss, and the FACTS establishment cost

TABLE 4. Imulation results for objective function values and Optimum control variables for scenario three (SVC- TCSC).

Control Variable & Objective	Min.	Max.	SLR				DLR			
			Best MSL	Best Losses	Best Cost	BCS	Best MSL	Best Losses	Best Cost	BCS
P_{g_2} MW	20	80	79.49	74.35	80.00	80.00	65.05	76.05	71.56	72.31
P_{g_5} MW	15	50	50.00	46.06	50.00	50.00	49.97	46.16	45.36	48.41
P_{g_8} MW	10	35	34.23	33.27	32.38	33.26	34.73	34.42	34.52	34.88
P_{g_11} MW	10	30	30.00	23.79	29.65	28.43	28.65	27.448	28.591	29.217
P_{g_13} MW	12	40	12.00	20.79	40.00	21.95	21.91	19.82	27.27	25.96
V_{g_1} (pu)	0.95	1.10	1.032	1.061	1.053	1.059	1.049	1.018	1.048	1.08
V_{g_2} (pu)	0.95	1.10	1.032	1.042	1.048	1.047	1.05	1.037	1.066	1.078
V_{g_5} (pu)	0.95	1.10	0.999	1.032	1.041	1.042	1.032	0.998	1.026	1.014
V_{g_8} (pu)	0.95	1.10	1.001	1.041	1.0193	1.036	1.037	1.023	1.016	1.026
V_{g_11} (pu)	0.95	1.10	1.062	1.074	1.064	1.097	1.089	1.058	1.07	1.047
V_{g_13} (pu)	0.95	1.10	1.054	1.074	1.007	1.000	1.0588	1.045	0.986	1.047
$T_{6\text{-}9}$ (pu)	0.90	1.10	0.927	1.009	1.075	1.060	0.952	1.052	0.900	0.917
$T_{6\text{-}10}$ (pu)	0.90	1.10	0.901	0.900	0.900	0.9000	1.020	1.051	1.007	1.003
$T_{4\text{-}12}$ (pu)	0.90	1.10	1.098	1.006	1.023	1.027	1.005	0.954	0.996	0.936
$T_{27\text{-}28}$ (pu)	0.90	1.10	0.925	0.966	0.939	0.954	0.937	0.962	0.924	0.950
λ_f	1.0	1.50	1.28	1.01	1.13	1.16	1.29	1.01	1.09	1.32
MSL (%)			**128.0**	101.0	113.0	**116.0**	**129.0**	101.0	109.0	**132.0**
$\mathbb{E}$ [Loses (MW)]			7.54	**3.47**	4.86	**5.02**	7.55	**3.58**	5.38	**7.89**
ICX10^6 USD	-		4.52	6.32	**1.37**	**4.92**	5.64	3.92	**0.864**	**7.57**
SVC_1 (MVAr)	-100	100	-0.252	-21.28	-2.35	0.22	11.75	21.81	-3.35	-6.82
SVC_2 (MVAr)	-100	100	4.14	26.34	-1.14	-5.05	15.57	8.35	-0.098	28.60
SVC_3(MVAr)	-100	100	-5.010	3.78	2.38	4.41	-16.93	-13.01	0.528	23.22
Location Bus			10;19;30	4;12;28	25;17;30	28;22;30	15;20;24	10;17;29	3;16;7	28;17;7
TCSC (pu)	-0.2	0.8	-0.8	-0.78	-0.8	-0.79	-0.14	-0.16	-0.64	-0.33
Location Line			24-25	23-24	29-30	6-28	10-22	10-22	21-22	10-22

* Bold values represent the best results

for the BCS. In case of SLR, the SVCs are installed at in buses 28, 22, and 30, with ratings of size 0.22, - 5.05, and 4.412 MVAr, respectively and the TCSC are installed in line line number 41 between buses (6-28), with rating of – 0.79 pu, based on the BCS. In this case the MSL is 125%, the power losses is 5.02 MW and the TCSC establishment cost is US$ 4.92×10^6.

In case of DLR, the MSL is increased to 132% with the TCSC installed in line number 28, between buses (12-15), with rating of – 0.69 pu a along with SVCS are installed at in buses 14, 29, and 30, with ratings of size 0-6.82, 28.61, and 23.20 MVAr. The losses has increased to 7.89 MW and the establishment cost of the FACTS devices has increased to US$ 7.57×10^6.

C. COMPARISON OF THE THREE SCENARIOS

Table 5, displays a comparison of the BCS for all scenarios where the results indicate that the system loadability when using the TCSC is better as compared to the SVCs in case of SLR. However, in case of DLR, the use of SVCs leads to a higher value of system loadability. This is also shown in Fig. 10. The results also show that the loadability increases when considering the DLR as compared to SLR for all types of FACTS controllers. However, this increase is higher in case of using SVCs as compared to the TCSC. On the other hand, the power losses in case of DLR is increased as shown in Figure 11 for all types of FACTS devices. This is mainly due to the increase in the power flowing in different lines of the system as compared to SLR case. Regarding the FACTS

TABLE 5. Comparison of BCS for study Scenarios 1,2 and 3.

Objective& Parameter	Without FACTS		SVC		TCSC		SVC-TCSC	
	SLR	DLR	SLR	DLR	SLR	DLR	SLR	DLR
MSL (%)	112.0	123.0	117.0	137.0	125.0	130.0	116.0	132.0
𝔼 [Loses (MW)]	4.13	5.93	5.73	9.12	6.46	7.06	5.02	7.89
ICX10^6 USD	-	-	0.814	5.11	2.76	3.107	4.92	7.57
SVC1 (MVAr)	-	-	2.72	16.24	-	-	0.25	-6.82
SVC2 (MVAr)	-	-	2.81	24.93	-	-	-5.05	28.06
SVC3 (MVAr)	-	-	-1.57	1.03	-	-	4.41	23.22
SVC Location Bus	-	-	30;14;4	18;12;22			28;22;30	28;17;7
TCSC (pu)	-	-	-	-	-0.72	-0.69	-0.79	-0.33
TCSC Location Line			-	-	10-20	12-15	6-28	10-22

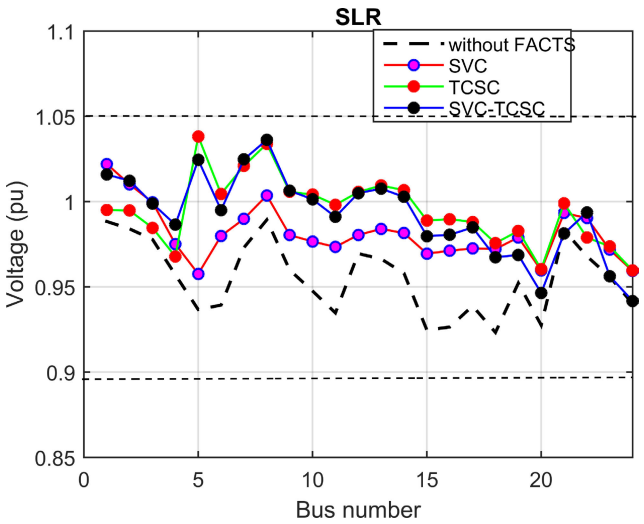

FIGURE 12. Load buses voltage profiles for the BCS for SLR.

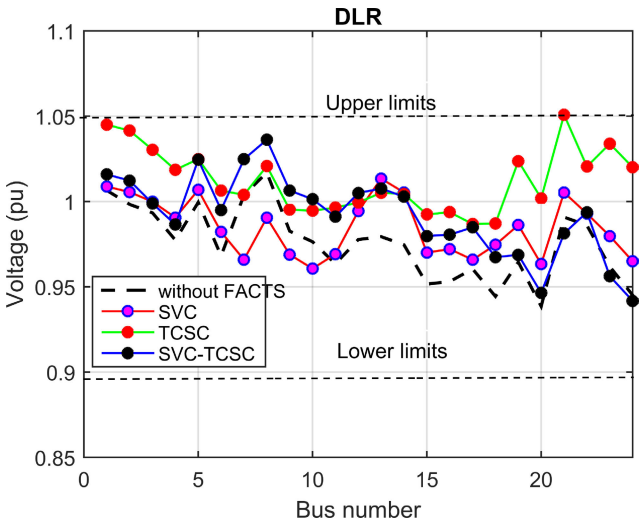

FIGURE 13. Load buses voltage profiles for the BCS for DLR.

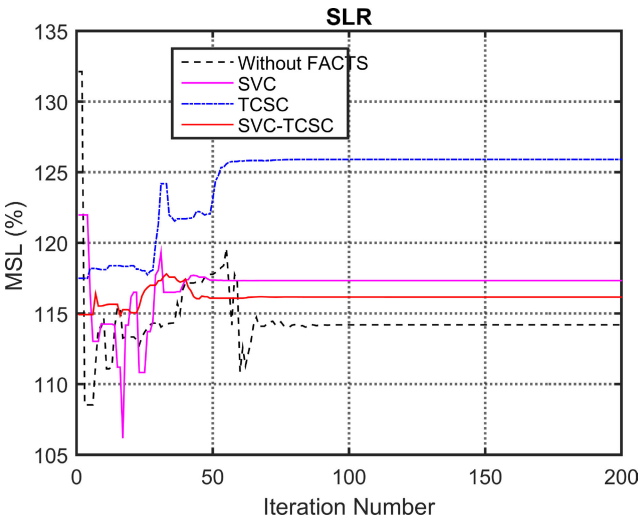

FIGURE 14. Convergence of BCS system loadability for SLR.

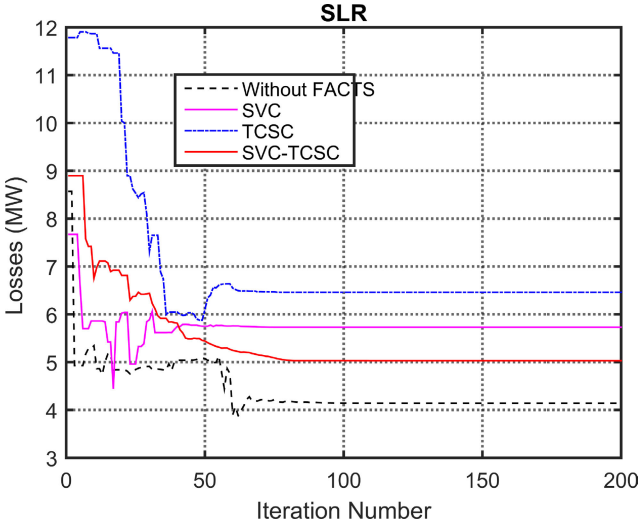

FIGURE 15. Convergence of BCS of power losses (MW) for SLR.

devices costs, it is clear that the use of DLR increases the cost as the size of the FACTS controllers has to be increased to accommodate the additional loadability of the system. The least increase in the cost is for the case of the TCSC which also corresponds to the least increase in the system loadability and power losses. Accordingly, it can be

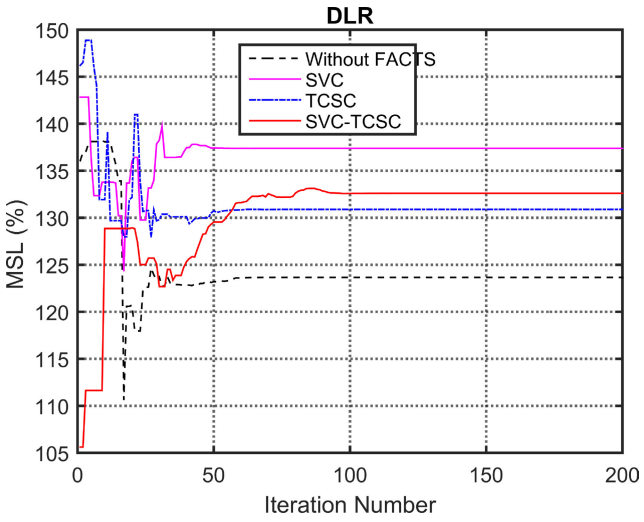

FIGURE 16. Convergence of BCS system loadability for DLR.

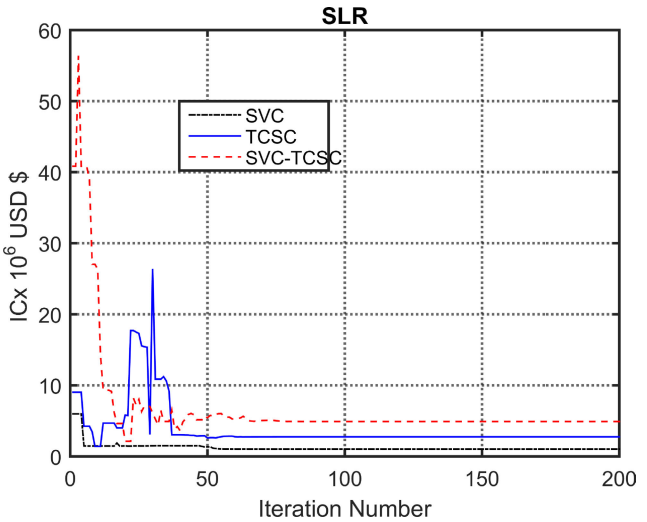

FIGURE 18. Convergence of BCS cos of FACTS USD for SLR.

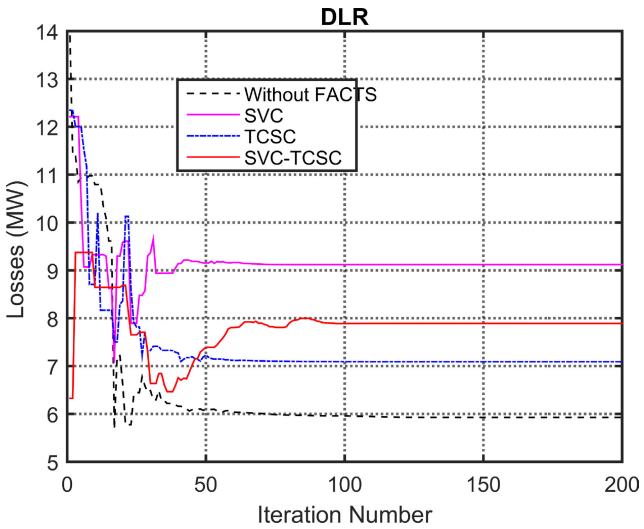

FIGURE 17. Convergence of BCS of power losses (MW) for DLR.

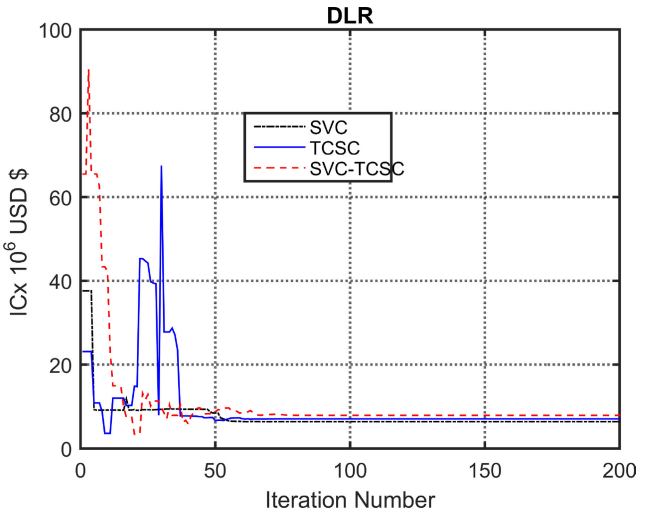

FIGURE 19. Convergence of BCS cos of FACTS USD for DLR.

concluded based on the system under study that the DLR has a higher impact in case of using the SVCs. Also, it can be observed from tabulated results no solution can dominate others offer all objective function. The voltage profiles corresponding to the BCS for all types of FACTS devices in case of SLR and DLR are shown in Fig. 12 and 13.

IX. APPROACH ASSESSMENT

The variation of best compromise solution (BCS) for the active power loss, MSL and the FACTS establishment cost versus the number of iterations for the SLR and DLR are presented in Fig. 14 to Fig. 19. The figures show that the solution for all cases converge at around 100 iterations. Hence, the proposed optimization approach shows fast convergence. Moreover, the convergence characteristics are not monotonic most likely due to the existence of best compromise solution (BCS). In each iteration, there are several non-dominated solutions and one of them has been selected as the BCS considering Equations (44) to (45). In the following iteration, however, another solution might be selected as the BCS, and therefore, a non-monotonic convergence may occur. It can be seen that after 200 iterations, all objective function settles to a fixed value.

X. CONCLUSION

This article uses two promising and effective technologies including FACTS controller and DLR, which are expected to improve congestion mitigation performance and contribute to the effective use of transmission networks. Therefore, this article introduced an effective and simple methodology for choosing the ideal capacity and location of FACTS controllers for networks with a high penetration of wind generation. The allocation of FACTS controllers is presented as an MOP. The objective functions taken into consideration simultaneously in the study were the maximization of network

loadability, the minimization of expected network losses, and the minimization of the FACTS controller installation cost. In this study, wind generation and load demand were considered uncertainties that were modeled using the PEM while seeking optimum allocation of FACTS controllers. The effectiveness of the proposed method was studied by applying it to the modified IEEE 30-bus system and it was solved using (MOTLBO+2PEM). Simulation results have shown that by incorporating DLR, the utilization of the transmission system could be improved and the amount of power could be increased compared to the outcomes achieved when these limits were constant. Addressing results in a more general note, it is demonstrated that DLR integration in the power grid can avoid building new transmission lines, solving some of the first grid problems due to RES generation development rapid growth. Thus, the use of FACTS controllers and DLR together complement each other and lead to enhancement of power system performance.

REFERENCES

[1] *Global Wind Report 2018*, Global Wind Energy Council, Brussels, Belgium, 2018.

[2] *Energy Policy Act of 2005*, Environ. Protection Act, US Congr., Washington, DC, USA, 2005.

[3] Y. Li, B. Hu, K. Xie, L. Wang, Y. Xiang, R. Xiao, and D. Kong, "Day-ahead scheduling of power system incorporating network topology optimization and dynamic thermal rating," *IEEE Access*, vol. 7, pp. 35287–35301, 2019.

[4] J. Teh, C.-M. Lai, N. A. Muhamad, C. A. Ooi, Y.-H. Cheng, M. A. A. M. Zainuri, and M. K. Ishak, "Prospects of using the dynamic thermal rating system for reliable electrical networks: A review," *IEEE Access*, vol. 6, pp. 26765–26778, 2018.

[5] S. Karimi, P. Musilek, and A. M. Knight, "Dynamic thermal rating of transmission lines: A review," *Renew. Sustain. Energy Rev.*, vol. 91, pp. 600–612, Aug. 2018.

[6] P. Kotsampopoulos, P. Georgilakis, D. T. Lagos, V. Kleftakis, and N. Hatziargyriou, "FACTS providing grid services: Applications and testing," *Energies*, vol. 12, no. 13, p. 2554, Jul. 2019.

[7] F. H. Gandoman, A. Ahmadi, A. M. Sharaf, P. Siano, J. Pou, B. Hredzak, and V. G. Agelidis, "Review of FACTS technologies and applications for power quality in smart grids with renewable energy systems," *Renew. Sustain. Energy Rev.*, vol. 82, pp. 502–514, Feb. 2018.

[8] B. Singh and R. Kumar, "A comprehensive survey on enhancement of system performances by using different types of FACTS controllers in power systems with static and realistic load models," *Energy Rep.*, vol. 6, pp. 55–79, Nov. 2020.

[9] S. Sreedharan, T. Joseph, S. Joseph, C. V. Chandran, J. Vishnu, and V. Das, "Power system loading margin enhancement by optimal STATCOM integration—A case study," *Comput. Electr. Eng.*, vol. 81, Jan. 2020, Art. no. 106521.

[10] N. Wang, J. Li, W. Hu, B. Zhang, Q. Huang, and Z. Chen, "Optimal reactive power dispatch of a full-scale converter based wind farm considering loss minimization," *Renew. Energy*, vol. 139, pp. 292–301, Aug. 2019.

[11] S. Gasperic and R. Mihalic, "Estimation of the efficiency of FACTS devices for voltage-stability enhancement with PV area criteria," *Renew. Sustain. Energy Rev.*, vol. 105, pp. 144–156, May 2019.

[12] B. Singh and G. Agrawal, "Enhancement of voltage profile by incorporation of SVC in power system networks by using optimal load flow method in MATLAB/simulink environments," *Energy Rep.*, vol. 4, pp. 418–434, Nov. 2018.

[13] V. Durković and A. S. Savić, "ATC enhancement using TCSC device regarding uncertainty of realization one of two simultaneous transactions," *Int. J. Electr. Power Energy Syst.*, vol. 115, Feb. 2020, Art. no. 105497.

[14] M. R. Aghaebrahimi, R. K. Golkhandan, and S. Ahmadnia, "Localization and sizing of FACTS devices for optimal power flow in a system consisting wind power using HBMO," in *Proc. 18th Medit. Electrotech. Conf. (MELECON)*, Apr. 2016, pp. 1–7.

[15] S. R. Salkuti and S.-C. Kim, "Congestion management using multi-objective glowworm swarm optimization algorithm," *J. Electr. Eng. Technol.*, vol. 14, no. 4, pp. 1565–1575, 2019.

[16] M. Nadeem, K. Imran, A. Khattak, A. Ulasyar, A. Pal, M. Z. Zeb, A. N. Khan, and M. Padhee, "Optimal placement, sizing and coordination of FACTS devices in transmission network using whale optimization algorithm," *Energies*, vol. 13, no. 3, p. 753, Feb. 2020.

[17] S. O. Faried, R. Billinton, and S. Aboreshaid, "Probabilistic technique for sizing FACTS devices for steady-state voltage profile enhancement," *IET Gener., Transmiss. Distrib.*, vol. 3, no. 4, pp. 385–392, 2009.

[18] S. Galloway, I. Elders, G. Burt, and B. Sookananta, "Optimal flexible alternative current transmission system device allocation under system fluctuations due to demand and renewable generation," *IET Gener., Transmiss. Distrib.*, vol. 4, no. 6, pp. 725–735, 2010.

[19] A. Hussain, M. Amin, R. D. Khan, and F. A. Chaudhry, "Optimal allocation of flexible AC transmission system controllers in electric power networks," *INAE Lett.*, vol. 3, no. 1, pp. 41–64, Mar. 2018.

[20] B. Bhattacharyya and S. Kumar, "Loadability enhancement with FACTS devices using gravitational search algorithm," *Int. J. Electr. Power Energy Syst.*, vol. 78, pp. 470–479, Jun. 2016.

[21] M. Sedighizadeh, H. Faramarzi, M. M. Mahmoodi, and M. Sarvi, "Hybrid approach to FACTS devices allocation using multi-objective function with NSPSO and NSGA-II algorithms in fuzzy framework," *Int. J. Electr. Power Energy Syst.*, vol. 62, pp. 586–598, Nov. 2014.

[22] S. Galvani, M. T. Hagh, M. B. B. Sharifian, and B. Mohammadi-Ivatloo, "Multiobjective predictability-based optimal placement and parameters setting of UPFC in wind power included power systems," *IEEE Trans. Ind. Informat.*, vol. 15, no. 2, pp. 878–888, Feb. 2019.

[23] F. Qiu and J. Wang, "Distributionally robust congestion management with dynamic line ratings," *IEEE Trans. Power Syst.*, vol. 30, no. 4, pp. 2198–2199, Jul. 2015.

[24] J. Teh, C.-M. Lai, and Y.-H. Cheng, "Improving the penetration of wind power with dynamic thermal rating system, static VAR compensator and multi-objective genetic algorithm," *Energies*, vol. 11, no. 4, p. 815, Apr. 2018.

[25] A. Safdarian, M. Z. Degefa, M. Fotuhi-Firuzabad, and M. Lehtonen, "Benefits of real-time monitoring to distribution systems: Dynamic thermal rating," *IEEE Trans. Smart Grid*, vol. 6, no. 4, pp. 2023–2031, Jul. 2015.

[26] J. Teh and I. Cotton, "Reliability impact of dynamic thermal rating system in wind power integrated network," *IEEE Trans. Rel.*, vol. 65, no. 2, pp. 1081–1089, Jun. 2016.

[27] J. Zhan, W. Liu, and C. Y. Chung, "Stochastic transmission expansion planning considering uncertain dynamic thermal rating of overhead lines," *IEEE Trans. Power Syst.*, vol. 34, no. 1, pp. 432–443, Jan. 2019.

[28] H. Park, Y. G. Jin, and J.-K. Park, "Stochastic security-constrained unit commitment with wind power generation based on dynamic line rating," *Int. J. Electr. Power Energy Syst.*, vol. 102, pp. 211–222, Nov. 2018.

[29] H. Abderazek, A. R. Yildiz, and S. Mirjalili, "Comparison of recent optimization algorithms for design optimization of a cam-follower mechanism," *Knowl.-Based Syst.*, vol. 191, Mar. 2020, Art. no. 105237.

[30] A. K. Shukla, P. Singh, and M. Vardhan, "An adaptive inertia weight teaching-learning-based optimization algorithm and its applications," *Appl. Math. Model.*, vol. 77, pp. 309–326, Jan. 2020.

[31] R. V. Rao, V. J. Savsani, and D. P. Vakharia, "Teaching–learning-based optimization: A novel method for constrained mechanical design optimization problems," *Comput.-Aided Des.*, vol. 43, no. 3, pp. 303–315, Mar. 2011.

[32] R. V. Rao, V. J. Savsani, and D. P. Vakharia, "Teaching–learning-based optimization: An optimization method for continuous non-linear large scale problems," *Inf. Sci.*, vol. 183, no. 1, pp. 1–15, Jan. 2012.

[33] M. Ghasemi, M. Taghizadeh, S. Ghavidel, J. Aghaei, and A. Abbasian, "Solving optimal reactive power dispatch problem using a novel teaching-learning-based optimization algorithm," *Eng. Appl. Artif. Intell.*, vol. 39, pp. 100–108, Mar. 2015.

[34] J. Nayak, B. Naik, G. Chandrasekhar, and H. Behera, "A survey on teaching-learning-based optimization algorithm: Short Journey from 2011 to 2017," in *Computational Intelligence in Data Mining*. Singapore: Springer, 2019, pp. 739–758.

[35] F. Zou, D. Chen, and Q. Xu, "A survey of teaching-learning-based optimization," *Neurocomputing*, vol. 335, pp. 366–383, Mar. 2019.

[36] V. K. Patel and V. J. Savsani, "A multi-objective improved teaching–learning based optimization algorithm (MO-ITLBO)," *Inf. Sci.*, vol. 357, pp. 182–200, Aug. 2016.

[37] M. Aien, A. Hajebrahimi, and M. Fotuhi-Firuzabad, "A comprehensive review on uncertainty modeling techniques in power system studies," *Renew. Sustain. Energy Rev.*, vol. 57, pp. 1077–1089, May 2016.
[38] P. P. Verma, D. Srinivasan, K. S. Swarup, and R. Mehta, "A review of uncertainty handling techniques in smart grid," *Int. J. Uncertainty, Fuzziness Knowl.-Based Syst.*, vol. 26, no. 3, pp. 345–378, Jun. 2018.
[39] S. Xia, X. Luo, K. W. Chan, M. Zhou, and G. Li, "Probabilistic transient stability constrained optimal power flow for power systems with multiple correlated uncertain wind generations," *IEEE Trans. Sustain. Energy*, vol. 7, no. 3, pp. 1133–1144, Jul. 2016.
[40] A. R. Jordehi, "How to deal with uncertainties in electric power systems? A review," *Renew. Sustain. Energy Rev.*, vol. 96, pp. 145–155, Nov. 2018.
[41] M. El-Azab, W. A. Omran, S. F. Mekhamer, and H. E. A. Talaat, "A probabilistic multi-objective approach for FACTS devices allocation with different levels of wind penetration under uncertainties and load correlation," *Int. J. Electr. Comput. Eng.*, vol. 10, no. 4, p. 3898, Aug. 2020.
[42] Y. Li, Z. Yang, G. Li, D. Zhao, and W. Tian, "Optimal scheduling of an isolated microgrid with battery storage considering load and renewable generation uncertainties," *IEEE Trans. Ind. Electron.*, vol. 66, no. 2, pp. 1565–1575, Feb. 2019.
[43] F. Teng, R. Dupin, A. Michiorri, G. Kariniotakis, Y. Chen, and G. Strbac, "Understanding the benefits of dynamic line rating under multiple sources of uncertainty," *IEEE Trans. Power Syst.*, vol. 33, no. 3, pp. 3306–3314, May 2018.
[44] M. Nick, O. Alizadeh-Mousavi, R. Cherkaoui, and M. Paolone, "Security constrained unit commitment with dynamic thermal line rating," *IEEE Trans. Power Syst.*, vol. 31, no. 3, pp. 2014–2025, May 2016.
[45] A. K. Kazerooni, J. Mutale, M. Perry, S. Venkatesan, and D. Morrice, "Dynamic thermal rating application to facilitate wind energy integration," in *Proc. IEEE Trondheim PowerTech*, Jun. 2011, pp. 1–7.
[46] A. Bücher and J. Segers, "On the maximum likelihood estimator for the generalized extreme-value distribution," *Extremes*, vol. 20, no. 4, pp. 839–872, Dec. 2017.
[47] M. Aien, M. Rashidinejad, and M. F. Firuz-Abad, "Probabilistic optimal power flow in correlated hybrid wind-PV power systems: A review and a new approach," *Renew. Sustain. Energy Rev.*, vol. 41, pp. 1437–1446, Jan. 2015.
[48] J. Zhang, G. Xiong, K. Meng, P. Yu, G. Yao, and Z. Dong, "An improved probabilistic load flow simulation method considering correlated stochastic variables," *Int. J. Electr. Power Energy Syst.*, vol. 111, pp. 260–268, Oct. 2019.
[49] X. Li, J. Cao, and D. Du, "Probabilistic optimal power flow for power systems considering wind uncertainty and load correlation," *Neurocomputing*, vol. 148, pp. 240–247, Jan. 2015.
[50] H. Zhang and P. Li, "Probabilistic analysis for optimal power flow under uncertainty," *IET Generat., Transmiss. Distrib.*, vol. 4, no. 5, pp. 553–561, May 2010.
[51] Y. Che, X. Wang, X. Lv, and Y. Hu, "Probabilistic load flow using improved three point estimate method," *Int. J. Electr. Power Energy Syst.*, vol. 117, May 2020, Art. no. 105618.
[52] S. M. Mohseni-Bonab, A. Rabiee, B. Mohammadi-Ivatloo, S. Jalilzadeh, and S. Nojavan, "A two-point estimate method for uncertainty modeling in multi-objective optimal reactive power dispatch problem," *Int. J. Electr. Power Energy Syst.*, vol. 75, pp. 194–204, Feb. 2016.
[53] M. B. Shafik, H. Chen, G. I. Rashed, and R. A. El-Sehiemy, "Adaptive multi objective parallel seeker optimization algorithm for incorporating TCSC devices into optimal power flow framework," *IEEE Access*, vol. 7, pp. 36934–36947, 2019.
[54] C. A. C. Coello, "Theoretical and numerical constraint-handling techniques used with evolutionary algorithms: A survey of the state of the art," *Comput. Methods Appl. Mech. Eng.*, vol. 191, nos. 11–12, pp. 1245–1287, Jan. 2002.
[55] H. Jain and K. Deb, "An evolutionary many-objective optimization algorithm using reference-point based nondominated sorting approach, part II: Handling constraints and extending to an adaptive approach," *IEEE Trans. Evol. Comput.*, vol. 18, no. 4, pp. 602–622, Aug. 2014.
[56] M. Saravanan, S. M. R. Slochanal, P. Venkatesh, and J. P. S. Abraham, "Application of particle swarm optimization technique for optimal location of FACTS devices considering cost of installation and system loadability," *Electr. Power Syst. Res.*, vol. 77, nos. 3–4, pp. 276–283, Mar. 2007.
[57] F. Zou, L. Wang, X. Hei, D. Chen, and B. Wang, "Multi-objective optimization using teaching-learning-based optimization algorithm," *Eng. Appl. Artif. Intell.*, vol. 26, no. 4, pp. 1291–1300, Apr. 2013.
[58] H. A. Hashim and M. A. Abido, "Location management in LTE networks using multi-objective particle swarm optimization," *Comput. Netw.*, vol. 157, pp. 78–88, Jul. 2019.
[59] O. Alsac and B. Stott, "Optimal load flow with steady-state security," *IEEE Trans. Power App. Syst.*, vol. PAS-93, no. 3, pp. 745–751, May 1974.
[60] R. D. Zimmerman, C. E. Murillo-Sánchez, and R. J. Thomas, "MATPOWER: Steady-state operations, planning, and analysis tools for power systems research and education," *IEEE Trans. Power Syst.*, vol. 26, no. 1, pp. 12–19, Feb. 2011.

MAHROUS EL-AZAB was born in Egypt, in 1971. He received the B.Sc. and M.Sc. degrees in electrical power and machine department from the Faculty of Engineering, Cairo University, Cairo, Egypt, in 1996 and 2004, respectively. He is currently pursuing the Ph.D. degree with the Faculty of Engineering, Ain Shams University, Cairo. He is also working full time at Osman Group Co. His research interests include power systems operation, renewable energy systems, energy storage systems, and wind energy.

WALID A. OMRAN received the B.Sc. and M.Sc. degrees in electrical engineering from Ain Shams University, Cairo, Egypt, in 1998 and 2005, respectively, and the Ph.D. degree from the Department of Electrical and Computer Engineering, University of Waterloo, Canada, in 2010. He is currently an Associate Professor with the Faculty of Engineering and Technology, Future University, Egypt (on leave from Ain Shams University). His research interests include the planning and operation of smart grids, integration of renewable energy systems, and energy storage systems.

SAID FOUAD MEKHAMER was born in Egypt, in 1964. He received the B.Sc. and M.Sc. degrees in electrical engineering from Ain Shams University, Cairo, Egypt, and the Ph.D. degree in electrical engineering from Ain Shams University, with joint supervision from Dalhousie University, Halifax, NS, Canada, in 2002. He is currently a Professor with the Department of Electric Power and Machines, Ain Shams University. He is also a Professor with Future University in Egypt (FUE), Cairo. He is on leave from Ain Shams University. His research interests include power system analysis, power system protection, and applications of AI in power systems.

HOSSAM E. A. TALAAT received the B.Sc. and M.Sc. degrees (Hons.) from Ain Shams University, Cairo, Egypt, in 1975 and 1980, respectively, and the Ph.D. degree (Tres Honorable) from the University of Grenoble, France, in 1986. He is currently a Professor of electrical power systems and the Head of the Electrical Engineering Department, Future University in Egypt (FUE), Cairo, Egypt. He is on leave from Ain Shams University, Cairo. He is a member of a number of scientific and technical committees. He has supervised many M.Sc. and Ph.D. theses in the field of power system control and protection. He has taught many undergraduate and graduate courses in this field. He has authored or coauthored more than 80 technical papers. He is interested in many research areas such as the application of artificial intelligence techniques (neural networks, knowledge-based systems, genetic algorithms, and fuzzy logic) to power system analysis, control, and protection; real-time applications to electrical power systems and machines; as well as the application of optimal and adaptive control techniques for the enhancement of power system stability.